*ICIC Express Letters*
Volume **18**, Number **2**, February **2024**
 ISSN 1881-803X
pp. **183–191**

# FADING-WEIGHT ROBUST MODEL PREDICTIVE CONTROL FOR HYBRID ENERGY STORAGE SYSTEMS

Weilin Yang, Wanlin Shen, Guanyang Hu, Tinglong Pan and Dezhi Xu*

School of Internet of Things Engineering
Jiangnan University
No. 1800, Lihu Avenue, Wuxi 214122, P. R. China
{ wlyang; tlpan }@jiangnan.edu.cn; { 6211925002; guanyanghu }@stu.jiangnan.edu.cn
*Corresponding author: xudezhi@jiangnan.edu.cn

Received May 2023; accepted July 2023

Abstract. *In the context of controlling hybrid energy storage systems (HESSs), dealing with model mismatch arising from parameter inaccuracy has emerged as a major challenge. This paper presents a novel approach to addressing this challenge through the use of a robust model predictive control (RMPC) strategy based on fading-weight cost function. Specifically, the fading-weight cost function has been proposed to place more emphasis on the short-term predictive control capability of the controller. This attribute is especially relevant for cases of model mismatch. The proposed approach also integrates a moving horizon estimation (MHE) mechanism to enhance the controller's ability to suppress disturbances. The MHE algorithm achieves this goal by continuously estimating and updating the upper bound of the disturbance based on the state of the system at each moment. Simulation results confirm the effectiveness and superiority of the proposed RMPC strategy for HESS control.*
**Keywords:** Hybrid energy storage system, Robust model predictive control, Fading-weight cost function, Moving horizon estimation, Model mismatch

1. **Introduction.** In recent years, there has been a significant focus on energy storage technology both domestically and internationally [1, 2, 3]. While batteries continue to be the primary energy storage carrier for existing devices due to their high energy density, they are limited by their storage mechanism. This results in low power density, few cycles, and unsuitability for high-power charging and discharging, as well as frequent charging and discharging occasions. Supercapacitors (SCs), on the other hand, have fast response speed, low energy density, strong power output capacity, and long cycle life. Hybrid energy storage systems (HESSs), which combine both batteries and SCs, can leverage the high power density of SCs and high energy density of batteries. This enhances the efficiency of the entire system and extends battery service life. Consequently, HESS solutions have gained wider acceptance and commendable applications across various fields such as multi-area interconnected power systems [4], electric vehicles [5], and photovoltaic systems [6].

The integration of two distinct energy storage device characteristics renders the control design complex. Addressing multi-constraint control problems and achieving multi-objective optimization in such scenarios, require advanced control algorithms based on models. Model predictive control (MPC) is an algorithm of this nature that has gained widespread use in the control of HESSs due to its advantages. It is important to note that for achieving optimal prediction performance, accurate modeling of HESSs is necessary. A mismatch between the prediction model and the controlled system could significantly decrease the MPC's performance.

DOI: 10.24507/icicel.18.02.183

Some scholars have directed their efforts towards enhancing the precision of system models. In particular, voltage sensors were integrated into the battery and SC as studied in [7]. A more sophisticated battery model was employed with the aim of enhancing the accuracy of the system model. The MPC strategy was developed based on a linear state-space model, which regulated the operation of an HESS under constraints. The approach facilitates power distribution, and extends the battery life. Despite the improvement in the model's accuracy achieved by the above approach, the default system parameter retains static accuracy, and hence, exhibits certain limitations. In this context, a novel MPC strategy was introduced in [8], which is founded on a linear parameter-varying (LPV) model that accommodates variations in battery parameters across its state of charge. The proposed LPV prediction model outperforms prevailing linear time-invariant prediction models in terms of prediction accuracy, albeit at the expense of increased computational burden.

Furthermore, there is a growing body of literature that emphasizes the importance of improving controller robustness to minimize the impact of model mismatch on system behavior. For instance, in [9], researchers proposed a robust model predictive control (RMPC) strategy for the control of an HESS that can account for various operational constraints and model uncertainties. Notably, there is a significant gap in the research on model mismatch problems from a controller perspective, which presents ample opportunities for further exploration. In this study, we propose a novel fading-weight cost function for RMPC controller design and demonstrate its efficacy. To the best of our knowledge, this work is the first to introduce the fading-weight cost function in state-space model based RMPC strategy design. Besides, we propose a moving horizon estimation (MHE) approach for estimating the upper-bound of the disturbance.

In summary, this study makes several significant contributions. First, it proposes a fading-weight cost function and corresponding RMPC controller that prioritize short-term predictive control performance and address the issue of model mismatch caused by the time-varying parameters of the HESS. Second, the study introduces an MHE technique that estimates the upper bound of the disturbance based on real-time system state, leading to improved disturbance suppression capabilities. These contributions have the potential to enhancing the effectiveness and reliability of control strategies for HESSs. The simulation results show that the proposed control strategy has good control performance for the HESS, especially in the case of disturbance or model mismatch.

The remaining sections are organized as follows. In Section 2, the composition and modeling process of an HESS are introduced. In Section 3, the controller design is presented and the MHE method is described. The results of simulation are given in Section 4. A summary is given for this paper in Section 5.

## 2. **Modeling of the Hybrid Energy Storage System.**

In this section, we firstly introduce the overall structure and working principle of the HESS. Then, its state-space averaged model is derived.

### 2.1. **Description of the HESS.**

The circuit diagram of the HESS we studied is shown in Figure 1. It contains two bidirectional direct current-direct current (DC/DC) converters, a lithium battery and an SC. Two DC/DC converters are in parallel at both ends of the load, and each DC/DC converter is made up of two insulated gate bipolar transistors (IGBTs), a capacitor $C_i$, an inductor $L_i$, and a resistor $R_{Li}$, where $i = 1, 2$. The capacitors $C_1$ and $C_2$ are used to filter the high frequency portion produced by switching IGBTs, i.e., acting as a low pass filter. The loss of the inductors $L_1$ and $L_2$ is expressed by their connected resistors $R_{L1}$ and $R_{L2}$, respectively.

The commonly used internal resistance model is considered for the battery, which consists of an ideal voltage source $E_b$ and an equivalent resistance $R_b$ in series. An ideal

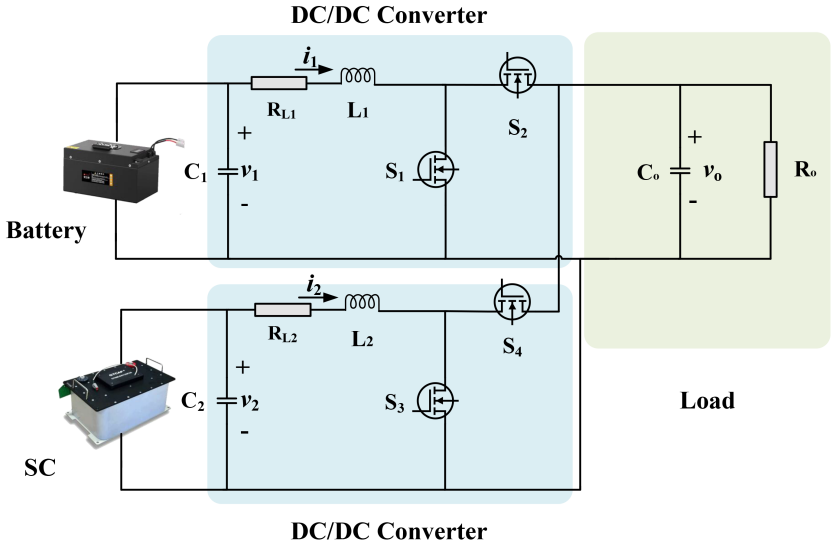


FIGURE 1. The hybrid energy storage system structure diagram

capacitor $C_{sc}$ and an equivalent resistor $R_{sc}$ in series form the simple RC model used for the SC. It is worth mentioning that the voltage drop of the SC under high current discharge is much slower than that of others, so the dynamic characteristics of the SC can be ignored. For this reason, the capacitor $C_{sc}$ is replaced with an ideal voltage source $E_{sc}$.

The IGBTs $S_1$ and $S_2$ in the DC/DC converter operate simultaneously, i.e., when one is turned on, the other is turned off. The IGBTs $S_3$ and $S_4$ operate in the same way. The duty cycles during which $S_1$ and $S_3$ are turned on are defined as $D_1$ and $D_2$, respectively. The on-resistance values of $S_1$, $S_2$, $S_3$, and $S_4$ are $R_{on1}$, $R_{on2}$, $R_{on3}$, and $R_{on4}$, respectively.

2.2. **Modeling of the HESS.** As shown in Figure 1, five variables are marked in the circuit, i.e., $v_1$, $v_2$, $i_1$, $i_2$ and $v_o$, and their average value in a switching cycle is defined as $\bar{v}_1$, $\bar{v}_2$, $\bar{i}_1$, $\bar{i}_2$ and $\bar{v}_o$. Below, we will derive the state-space averaged model for the HESS.

Define the status variable as $x = \begin{bmatrix}\bar{v}_1 & \bar{v}_2 & \bar{i}_1 & \bar{i}_2 & \bar{v}_o\end{bmatrix}^T$ and the control input vector as $u = [E_b \;\; E_{sc}]^T$. We can select any circuit variable of interest as the output, and this paper defines the output variable as $y = \begin{bmatrix}\bar{i}_1 & \bar{v}_o\end{bmatrix}^T$. From this, the fifth-order state-space model of the HESS is derived, as shown in Equation (1).

$$\dot{x} = A_c x + B_c u \tag{1a}$$

$$y = C_c x, \tag{1b}$$

where

$$A_c := \begin{bmatrix} -\frac{1}{R_b C_1} & 0 & -\frac{1}{C_1} & 0 & 0 \\ 0 & -\frac{1}{R_{sc} C_2} & 0 & -\frac{1}{C_2} & 0 \\ \frac{1}{L_1} & 0 & -\frac{R_{L1}+R_{on2}}{L_1} + D_1\frac{R_{on2}-R_{on1}}{L_1} & 0 & \frac{D_1-1}{L_1} \\ 0 & \frac{1}{L_2} & 0 & -\frac{R_{L2}+R_{on4}}{L_2} + D_2\frac{R_{on4}-R_{on3}}{L_2} & \frac{D_2-1}{L_2} \\ 0 & 0 & \frac{D_1-1}{C_o} & \frac{D_2-1}{C_o} & -\frac{1}{R_o C_o} \end{bmatrix},$$

$$B_c := \begin{bmatrix} \frac{1}{R_b C_1} & 0 \\ 0 & \frac{1}{R_{sc} C_2} \\ 0 & 0 \\ 0 & 0 \\ 0 & 0 \end{bmatrix}, \text{ and } C_c := \begin{bmatrix} 0 & 0 & 1 & 0 & 0 \\ 0 & 0 & 0 & 0 & 1 \end{bmatrix}.$$

After discretization, the discrete model is obtained as follows:

$$\begin{aligned} x(k+1) &= Ax(k) + Bu(k) \\ y(k) &= Cx(k), \end{aligned} \tag{2}$$

where $A$, $B$ and $C$ are the system matrices.

**Remark 2.1.** *The specific details of obtaining the state-space averaged model (1) are referred to* [10].

3. **Control Design.** This section discusses the proposed fading-weight RMPC controller and the MHE method. Specifically, the MHE method estimates the upper bound of the disturbance based on real-time disturbance to the system, and is applied to the design of the fading-weight RMPC controller. The proposed control strategy is shown in Figure 2.

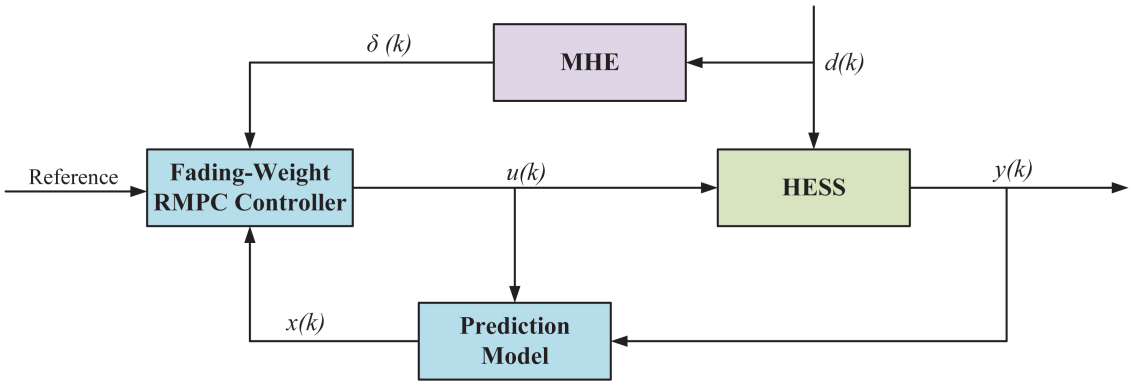


FIGURE 2. The structure diagram of the proposed control strategy

3.1. **Prediction model.** Considering modeling errors, external disturbances and other factors, the following prediction model is adopted for the state-space averaged model (2).

$$x(k+i+1|k) = Ax(k+i|k) + Bu(k+i|k) + d(k+i|k), \tag{3}$$

where $d \in R^q$ is the external disturbance. Moreover, control input is limited to $|u_j| \leq \bar{u}_j$, $j = 1, 2$, and the external disturbance satisfies the constraint $\|d\|^2 \leq \delta$, where scalar $\delta > 0$ is to be estimated online.

3.2. **Moving horizon estimation method.** In order to determine the value of $\delta$, an MHE approach is employed in this paper, which can update the value of $\delta$ according to the real-time system state. Specifically, we represent the disturbance as

$$d(k) = x(k) - \tilde{x}(k), \tag{4}$$

where $x(k)$ is the state of the system with external disturbance and $\tilde{x}(k)$ is the state of the system without external disturbance. Then, the disturbance constraint can be further expressed as

$$(x(k) - \tilde{x}(k))^T (x(k) - \tilde{x}(k)) \leq \delta. \tag{5}$$

We perform a minimization process, namely

$$\begin{aligned} &\min\ \delta \\ &\text{s.t. } \delta > 0. \end{aligned} \tag{6}$$

In this way, we can obtain the minimum value of $\delta$ at time $k$, i.e., $\delta^*(k)$. Similarly, at time $k-1$, there is also a minimum value of $\delta$, i.e., $\delta^*(k-1)$. The value of $\delta$ is assigned with $\delta^*(k)$ and used it in controller design, if the following condition is satisfied.

$$\delta^*(k-1) < \delta^*(k). \tag{7}$$

3.3. **RMPC ingredients.** We consider the following $H_\infty$-type fading-weight cost function.

$$J_\infty(k) = \sum_{i=0}^{\infty} \alpha^i \mathcal{L}(x(k+i|k), u(k+i|k), d(k+i|k)), \tag{8}$$

with the fading weight $\alpha^i$ and the state cost $\mathcal{L} := \|x\|_Q^2 + \|u\|_R^2 - \mu\|d\|^2$, where $\alpha \in [0,1]$ is a scalar, $Q > 0$ and $R > 0$ are constant positive definite matrices, and $\mu > 0$ is a scalar. To obtain an upper bound on the cost function, introduce a quadratic function $V(x) := x^{\mathrm{T}} P x$, where $P$ is a positive definite matrix, such that the following inequality holds for all $i \geq 0$.

$$\begin{aligned} &\alpha^{i+1} V(x(k+i+1|k)) - \alpha^i V(x(k+i|k)) \\ &\leq -\alpha^{i+1} \mathcal{L}(x(k+i|k), u(k+i|k), d(k+i|k)). \end{aligned} \tag{9}$$

Then, we need to derive the upper bound of the $H_\infty$-type fading-weight cost function (8) as follows:

$$\sum_{i=0}^{\infty} \alpha^i \mathcal{L}(x(k+i|k), u(k+i|k), d(k+i|k)) \leq V(x(k|k)), \tag{10}$$

where $V(x(k|k))$ is the desired upper bound. We minimize this upper bound by introducing a scalar $\gamma$,

$$\begin{aligned} &\min\ \gamma \\ &\text{s.t. } V(x(k|k)) \leq \gamma. \end{aligned} \tag{11}$$

On the basis of the Schur complement and the definition of $\Lambda := P^{-1}\gamma$, the constraint in Inequality (11) is equivalent as follows:

$$\begin{bmatrix} 1 & x(k|k)^{\mathrm{T}} \\ x(k|k) & \Lambda \end{bmatrix} \geq 0. \tag{12}$$

For future control inputs, the following linear feedback control law is employed.

$$u(k+i|k) = Kx(k+i|k), \quad i \geq 0. \tag{13}$$

Substituting Equation (13) into inequality (9), one has

$$\begin{aligned} &\|(A+BK)x(k+i|k) + d(k+i|k)\|_P^2 - \|x(k+i|k)\|_P^2 / \alpha \\ &\leq -\|x(k+i|k)\|_{(Q+K^{\mathrm{T}}RK)}^2 + \mu\|d\|^2. \end{aligned} \tag{14}$$

Based on Schur complement, a sufficient condition for Inequality (14) to hold can be obtained as follows:

$$\begin{bmatrix} -\Lambda/\alpha & * & * & * & * \\ 0 & -\zeta I & * & * & * \\ A\Lambda + BF & \gamma I & -\Lambda & * & * \\ Q\Lambda & 0 & 0 & -\gamma Q & * \\ RF & 0 & 0 & 0 & -\gamma R \end{bmatrix} \leq 0, \tag{15}$$

where $F := K\Lambda$, $\zeta := \mu\gamma$. Inequality (14) can be further written as follows:

$$\begin{aligned}&\|(A+BK)x(k+i|k)+d(k+i|k)\|_P^2-\|x(k+i|k)\|_P^2\\&\leq -\|x(k+i|k)\|_{(Q+K^{\mathrm{T}}RK)}^2+\mu\|d\|^2+\frac{1-\alpha}{\alpha}\|x(k+i|k)\|_P^2.\end{aligned}\tag{16}$$

It is required that

$$-\|x(k+i|k)\|_{(Q+K^{\mathrm{T}}RK)}^2+\mu\|d\|^2+\frac{1-\alpha}{\alpha}\|x(k+i|k)\|_P^2<0.\tag{17}$$

According to Schur complement, the sufficient condition of the above inequality can be obtained as follows,

$$\begin{bmatrix}-\gamma Q & \sqrt{\dfrac{1-\alpha}{\alpha}}\gamma I\\ * & -\Lambda\end{bmatrix}<0.\tag{18}$$

The new variable $\zeta$ represents the level of disturbance attenuation in input-to-state stable analysis. To ensure better control performance, a smaller value of $\mu$ is required. Since both $\mu$ and $\gamma$ are minimized, the optimization problem can be turned into

$$\begin{aligned}&\min\zeta\\&\text{s.t. }\gamma\leq\gamma_0,\end{aligned}\tag{19}$$

where $\gamma_0$ is an upper bound value of $\gamma$. The constraint (19) is used to ensure that the value of $\gamma$ does not increase.

Now it is time to consider the handling of input constraints. Applying the techniques presented in [11], the input constraint can be satisfied by the following linear matrix inequality.

$$\begin{bmatrix}Z & F\\ F^{\mathrm{T}} & \Lambda\end{bmatrix}\geq 0,\tag{20}$$

with $Z_{jj}\leq\bar{u}_j^2$, where $Z$ is a symmetric matrix.

Due to the existence of the disturbance, a robust positively invariant (RPI) set constraint [12] is supposed to be considered to ensure the recursive feasibility of online optimization problem solving. Based on the S-procedure, the RPI set can be guaranteed by the following sufficient conditions with a positive scalar $\lambda$.

$$\begin{bmatrix}\|A+BK\|_{P/\gamma}^2-P/\gamma & *\\ (P/\gamma)(A+BK) & P/\gamma\end{bmatrix}-\lambda\begin{bmatrix}-P/\gamma & *\\ 0 & 1/\delta I\end{bmatrix}\leq 0.\tag{21}$$

Using the Schur complement, the above inequality is equivalent to

$$\begin{bmatrix}(-1+\lambda)\Lambda & * & *\\ 0 & -\lambda/\delta I & *\\ A\Lambda+BF & I & -\Lambda\end{bmatrix}\leq 0.\tag{22}$$

To sum up, the optimization problem solved online is turned into

$$\begin{aligned}&\min_{\Lambda,F,\gamma,\zeta,\lambda}\zeta\\&\text{s.t. }(12),(15),(18),(19),(20),(22).\end{aligned}\tag{23}$$

4. **Simulations.** In this section, the proposed novel fading-weight RMPC strategy is applied to the HESS to achieve accurate control of battery current and load voltage, so as to demonstrate the effectiveness of the proposed strategy. The simulations are performed in MATLAB using the YALMIP toolbox [13] and SDPT3-4.0 toolbox [14]. As an illustration of the superiority of the proposed method, there will be a comparison with the $H_\infty$-type RMPC [15], which makes use of a traditional cost function.

Figure 3 shows the comparison of the proposed method with or without MHE method, in which the fading weight is $\alpha = 0.95$ and the disturbance added throughout is selected as $d(k) = \sin(k/4 - 1)/6 \cdot [1\ \ 1\ \ 1\ \ 1\ \ 1]^T$. Simulation results show that both of them are able to keep the HESS stable under the disturbed conditions. However, for the same disturbance, the proposed method has better disturbance suppression performance.

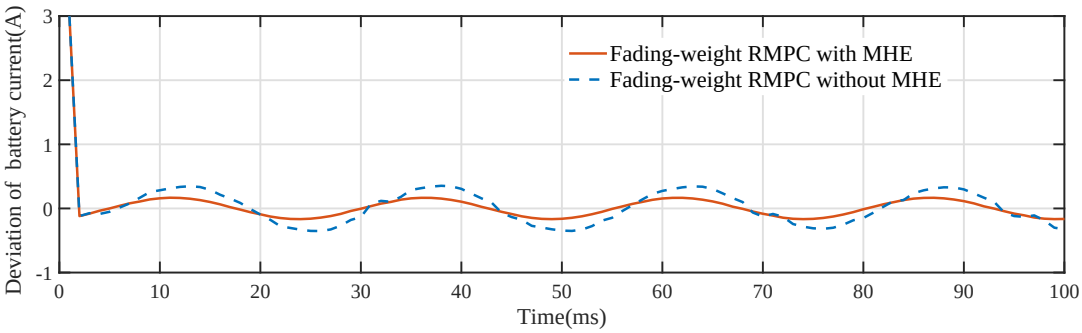


(a)

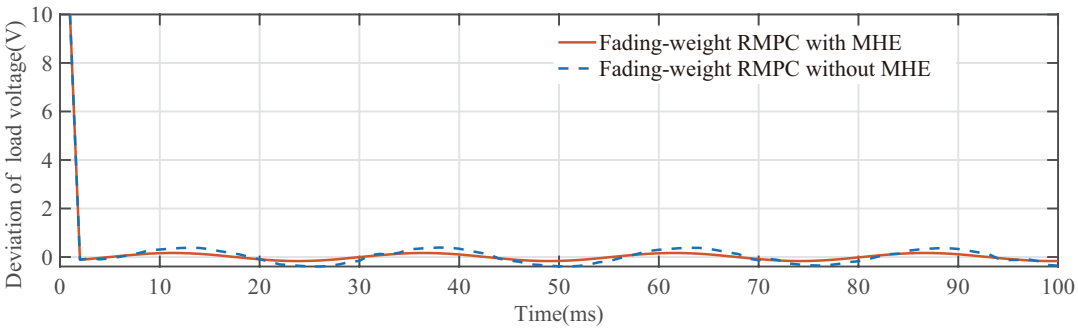


(b)

FIGURE 3. Comparison of the battery current and load voltage control performance between fading-weight RMPC with and without MHE method

To further demonstrate the superiority of the proposed fading-weight RMPC method, the model mismatch is considered, specifically, $R_{L2}$ changes from 0.114 Ω to 0.314 Ω. As shown in Figure 4, the proposed method can still achieve accurate control of battery current and load voltage under the condition of disturbance, where the fading weight is $\alpha = 0.8$ and the disturbance added throughout is selected as $d(k) = \sin(k/4 - 1)/10 \cdot [1\ \ 1\ \ 1\ \ 1\ \ 1]^T$. A comparison with the $H_\infty$-type RMPC approach using the traditional cost function is also given. As can be seen from Figure 4, in the case of model mismatch, the $H_\infty$-type RMPC method has poor control performance on the battery current, with a large overshoot at the initial phase, and the two methods have similar control performance on the load voltage.

5. **Conclusions.** In this paper, we propose a novel RMPC strategy for HESSs based on a fading-weight cost function. This approach is devised to enhance the control performance of the RMPC controller when faced with the model mismatch problem. Furthermore, we introduce a new technique for estimating the upper bound of the disturbance by means of an MHE method that utilizes the real-time system state. This estimation method is updated during operation to further improve the disturbance suppression capability for the controller. The simulations demonstrate the excellent performance of the proposed

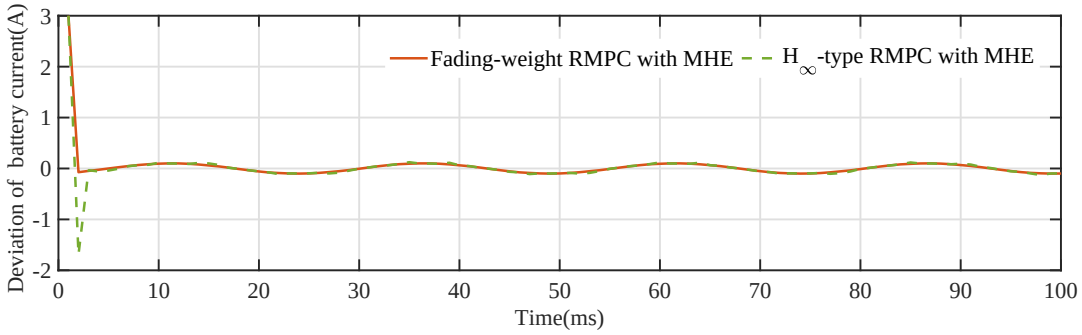


(a)

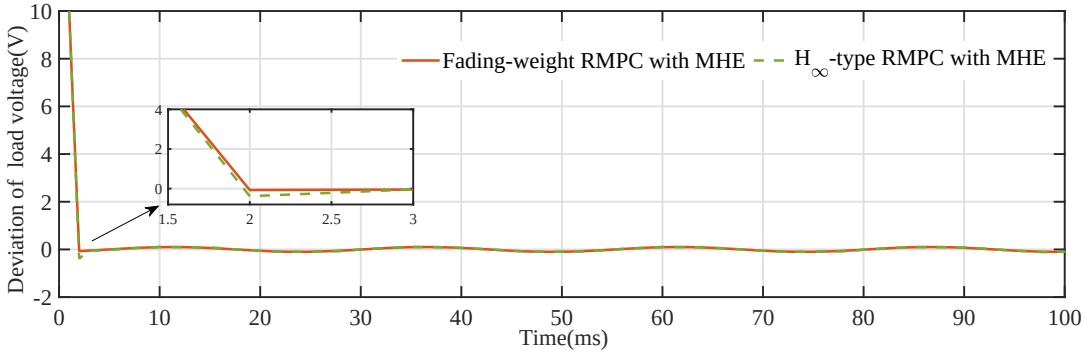


(b)

FIGURE 4. Comparison of the battery current and load voltage control performance between fading-weight RMPC and $H_\infty$-type RMPC method

method in terms of both disturbance suppression and model mismatch problem. Therefore, the proposed method could be a promising approach for controlling HESS under uncertainties. Our future work will be extending the relevant results to multiple interconnected HESSs.

**Acknowledgment.** This work is partially supported by the National Natural Science Foundation of China (Grant No. 62222307, No. 61973140). The authors also gratefully acknowledge the helpful comments and suggestions of the reviewers, which have improved the presentation.

## REFERENCES

[1] A. Kanchanaharuthai and E. Mujjalinvimut, Finite-time command filtered backstepping control design for power systems with superconducting magnetic energy storage system, *International Journal of Innovative Computing, Information and Control*, vol.17, no.3, pp.873-885, 2021.

[2] D. Yu, W. Zhang, J. Li et al., Disturbance observer-based prescribed performance fault-tolerant control for a multi-area interconnected power system with a hybrid energy storage system, *Energies*, vol.13, no.5, 2020.

[3] H. Xu and M. Shen, The control of lithium-ion batteries and supercapacitors in hybrid energy storage systems for electric vehicles: A review, *International Journal of Energy Research*, vol.45, no.15, pp.20524-20544, 2021.

[4] F. Zhu, X. Zhou, Y. Zhang et al., A load frequency control strategy based on disturbance reconstruction for multi-area interconnected power system with hybrid energy storage system, *Energy Reports*, vol.7, pp.8849-8857, 2021.

[5] S. F. da Silva, J. J. Eckert, F. C. Corrêa et al., Dual HESS electric vehicle powertrain design and fuzzy control based on multi-objective optimization to increase driving range and battery life cycle, *Applied Energy*, vol.324, 2022.

[6] F. N. Budiman, M. A. M. Ramli, A. H. Milyani et al., Stochastic optimization for the scheduling of a grid-connected microgrid with a hybrid energy storage system considering multiple uncertainties, *Energy Reports*, vol.8, pp.7444-7456, 2022.

[7] B. Hredzak, V. G. Agelidis and M. Jang, A model predictive control system for a hybrid battery-ultracapacitor power source, *IEEE Transactions on Power Electronics*, vol.29, no.3, pp.1469-1479, 2013.

[8] C. Jia, J. Cui, W. Qiao et al., Real-time model predictive control for battery-supercapacitor hybrid energy storage systems using linear parameter varying models, *IEEE Journal of Emerging and Selected Topics in Power Electronics*, 2021.

[9] T. Guo, Y. Liu, J. Zhao et al., A dynamic wavelet-based robust wind power smoothing approach using hybrid energy storage system, *International Journal of Electrical Power & Energy Systems*, vol.116, 2020.

[10] Q. Zhong, C. Xie, S. Jin et al., New optimal control algorithms for battery-supercapacitor HESS based on Wirtinger-based integral inequality, *IEEE Access*, vol.9, pp.17707-17716, 2021.

[11] M. V. Khlebnikov, B. T. Polyak and V. M. Kuntsevich, Optimization of linear systems subject to bounded exogenous disturbances: The invariant ellipsoid technique, *Automation and Remote Control*, vol.72, no.11, pp.2227-2275, 2011.

[12] F. Tahir and I. M. Jaimoukha, Robust positively invariant sets for linear systems subject to model-uncertainty and disturbances, *IFAC Proceedings Volumes*, vol.45, no.17, pp.213-217, 2012.

[13] A. K. Ravat, A. Dhawan and M. Tiwari, *LMI and YALMIP: Modeling and Optimization Toolbox in MATLAB*, Springer Singapore, 2021.

[14] K. C. Toh, M. J. Todd and R. H. Tütüncü, On the implementation and usage of SDPT3 – A MATLAB software package for semidefinite-quadratic-linear programming, version 4.0, *Handbook on Semidefinite, Conic and Polynomial Optimization*, pp.715-754, 2012.

[15] W. Yang, L. Jin, D. Xu et al., Event-triggered $H_\infty$-type robust model predictive control of linear systems with disturbances, *IEEE Access*, vol.7, pp.53859-53867, 2019.